Organometallics 1987, *6*, 799–805

Synthesis, Characterization, and Crystal Structure of $(\mu\text{-H})_2Ru_3(\mu_3\text{-}\eta^2\text{-CHC(O)OCH}_3)(CO)_9$, a Stabilized Intermediate in the Reductive Elimination of Hydrocarbons from Trimetallic Clusters[1]

Melvyn Rowen Churchill,* Thomas S. Janik, Timothy P. Duggan, and Jerome B. Keister*

Department of Chemistry, University at Buffalo, State University of New York, Buffalo, New York 14214

Received September 11, 1986

Pyrolysis of $(\mu\text{-H})_3Ru_3(\mu_3\text{-CCO}_2CH_3)(CO)_9$ at 70 °C produces $(\mu\text{-H})_2Ru_3(\mu_3\text{-}\eta^2\text{-CHC(O)OCH}_3)(CO)_9$ (56% yield), characterized by spectroscopic methods and by X-ray crystallography. The complex $(\mu\text{-H})_2Ru_3(\mu_3\text{-}\eta^2\text{-CHC(O)OCH}_3)(CO)_9$ crystallizes in the centrosymmetric triclinic space group $P\bar{1}$ (No. 2) with a = 11.357 (3) Å, b =12.427 (3) Å, c = 14.886 (4) Å, α = 73.989 (21)°, β = 69.581 (20)°, γ = 88.081 (20)°, V = 1885.4 (9) Å^3, and Z = 4. Diffraction data (Mo Kα, 2θ = 5–50°) were collected with a Syntex P2$_1$ automated four-circle diffractometer, and the structure was refined to R_F = 3.2% for all 6682 data (R_F = 2.3% for those 5586 data with $|F_o| > 6\sigma(|F_o|)$). There are two crystallographically independent (but chemically equivalent) molecules in the asymmetric unit. Each molecule consists of a triangular array of ruthenium atoms. The α-carbon atom of the $\mu_3\text{-}\eta^2\text{-CHC(O)OCH}_3$ ligand bridges ruthenium atoms Ru(1) and Ru(3) with Ru–**C** = 2.135 (4)–2.154 (4) Å, while the carbonyl oxygen of this ester group is coordinated to the third ruthenium atom, Ru(2) (Ru–**O** = 2.134 (3)–2.145 (3) Å). Each ruthenium atom is linked to three terminal carbonyl ligands, while the Ru(1)–Ru(3) and Ru(2)–Ru(3) bonds are bridged by hydride ligands. Variable-temperature ^{1}H and ^{13}C NMR spectra of $(\mu\text{-H})_2Ru_3(\mu_3\text{-}\eta^2\text{-CHC(O)OCH}_3)(CO)_9$ indicate that two hydride migration processes occur on the NMR time scale. Conversion of $(\mu\text{-H})_3Ru_3(\mu_3\text{-CCO}_2CH_3)(CO)_9$ to $(\mu\text{-H})_2Ru_3(\mu_3\text{-}\eta^2\text{-CHC(O)OCH}_3)(CO)_9$ involves reductive elimination of a single C–H bond and stabilization of the resulting unsaturated Ru atom by coordination of the acyl; complete elimination of methyl acetate is achieved by treatment of $(\mu\text{-H})_2Ru_3(\mu_3\text{-}\eta^2\text{-CHC(O)OCH}_3)(CO)_9$ with CO.

The mechanisms of hydride transfer and C–H reductive elimination from metal clusters are poorly understood and are potentially applicable as models for analogous processes on metal surfaces.[2] We recently have studied the mechanism of reductive elimination of CH_3X from $(\mu\text{-H})_3Ru_3(\mu_3\text{-CX})(CO)_9$ (X = Ph, Cl, CO_2CH_3) under CO,[3] a process requiring three reductive eliminations per molecule. During the course of this study Shapley and Strickland reported the synthesis of $H_2Os_3(CHCO_2CH_3)(CO)_9$ by pyrolysis of $H_3Os_3(CCO_2CH_3)(CO)_9$; on the basis of spectroscopic data the structure of the product was proposed to contain a coordinated acyl group.[4] Since this rearrangement is the first C–H reductive elimination in the series of three leading to desorption of methyl acetate from the cluster, we have investigated the pyrolysis reaction of the analogous Ru cluster. The stabilized alkylidene product $(\mu\text{-H})_2Ru_3(\mu_3\text{-}\eta^2\text{-CHC(O)OCH}_3)(CO)_9$ has been characterized by spectroscopic methods and by X-ray crystallography. Reaction of $(\mu\text{-H})_2Ru_3(\mu_3\text{-}\eta^2\text{-CHC(O)OCH}_3)(CO)_9$ with CO induces two more C–H reductive eliminations, completing the "desorption" process.

Experimental Section

General Data. $(\mu\text{-H})_3Ru_3(\mu_3\text{-CCO}_2CH_3)(CO)_9$ was prepared by a previously published procedure.[5] Infrared spectra of cyclohexane solutions were recorded on a Beckman 4250 spectrophotometer and were referenced with the 2138.5 cm^{-1} absorption due to cyclohexane. ^{1}H and ^{13}C NMR spectra were recorded on a JEOL FX-90Q spectrometer; Cr(acac)$_3$ (0.02 M) was added as a relaxation agent for the ^{13}C NMR spectra. Mass spectra were recorded at the Penn State Mass Spectrometer Center by Dr. R. Minard. Elemental analyses were obtained from Schwarzkopf Microanalytical Laboratories.

$(\mu\text{-H})_2Ru_3(\mu_3\text{-}\eta^2\text{-CHC(O)OCH}_3)(CO)_9$. A solution of $(\mu\text{-H})_3Ru_3(\mu_3\text{-CCO}_2CH_3)(CO)_9$ (50 mg, 0.079 mmol) in cyclohexane (50 mL) was heated at 70 °C in a 100-mL Schlenk flask under a nitrogen atmosphere. After 24 h the solution was evaporated to dryness on a rotary evaporator. The residue was separated by using thin-layer chromatography on silica eluting with hexanes. The product, a yellow band near the bottom of the plate, was extracted with dichloromethane–acetone (10:1 v/v), and evaporation yielded 28 mg (56%). An analytically pure sample was obtained by recrystallization from methanol.

Anal. Calcd for $C_{12}H_6O_{11}Ru_3$: C, 22.90; H, 0.96. Found: C, 22.68; H, 1.03. IR (C_6H_{12}): 2106 m, 2078 vs, 2054 vs, 2032 vs, 2017 s, 2006 vs, 1991 s, 1980 sh vw, 1955 vw, 1540 w cm^{-1}. ^{1}H NMR (CDCl$_3$, 22 °C): 3.98 (br s, 1 H, C*H*), 3.54 (s, 3 H, OC*H*$_3$), −13.04 (br, 1 H, Ru*H*Ru), −14.91 (br, 1 H, Ru*H*Ru). ^{1}H NMR (CDCl$_3$, −10 °C): 3.94 (br s, 1 H), 3.53 (s, 3 H), −13.03 (d, 1 H$_a$), −14.90 (br d, 1 H$_b$) ppm, J_{ab} = 3.1 Hz. ^{13}C NMR: see Table V and Results and Discussion. MS (EI): m/z 636 (^{104}Ru$_3$).

Collection of the X-ray Diffraction Data for $(\mu\text{-H})_2Ru_3(\mu_3\text{-}\eta^2\text{-CHC(O)OCH}_3)(CO)_9$. A red-brown crystal of approximate orthogonal dimensions 0.40 × 0.30 × 0.15 mm^3 was mounted along its extended axis in a thin-walled glass capillary and was aligned and centered on a Syntex P2$_1$ automated four-circle diffractometer. Determination of accurate unit cell dimensions and the crystal's orientation matrix were performed as described previously.[6] Details of this and of data collection are given in Table I.

A survey of the data set revealed no symmetry other than the Friedel condition ($\bar{1}$) and no systematic absences. The crystal therefore belongs to the triclinic class with space group $P1$ or $P\bar{1}$. The latter, centrosymmetric, possibility was confirmed by the successful solution of the structure in this higher symmetry space

---

[1] This paper constitutes part 12 of the series "Structural Studies on Ruthenium Carbonyl Hydrides". Recent previous parts include the following. (a) Part 7: Rahman, Z. A.; Beanan, L. R.; Bavaro, L. M.; Modi, S. P.; Keister, J. B.; Churchill, M. R. *J. Organomet. Chem.* **1984**, *263*, 75. (b) Part 8: Churchill, M. R.; Fettinger, J. C.; Keister, J. B. *Organometallics* **1985**, *4*, 1867. (c) Part 9: Churchill, M. R.; Fettinger, J. C.; Keister, J. B.; See, R. F.; Ziller, J. W. *Organometallics* **1985**, *4*, 2112. (d) Part 10: Churchill, M. R.; Ziller, J. W.; Keister, J. B. *J. Organomet. Chem.* **1985**, *297*, 93. (e) Part 11: Churchill, M. R.; Duggan, T. P.; Keister, J. B.; Ziller, J. W. *Acta Crystallogr., Sect. C: Cryst. Struct. Commun.*, in press.

[2] Muetterties, E. L.; Rhodin, T. N.; Band, E.; Brucker, C. F.; Pretzer, W. R. *Chem. Rev.* **1979**, *79*, 91.

[3] Duggan, T. P.; Muscatella, M. J.; Barnett, D. J.; Keister, J. B. *J. Am. Chem. Soc.* **1986**, *108*, 6076.

[4] Strickland, D. A. Ph.D. Thesis, University of Illinois, 1983.

[5] Keister, J. B.; Horling, T. L. *Inorg. Chem.* **1980**, *19*, 2304.

[6] Churchill, M. R.; Lashewycz, R. A.; Rotella, F. J. *Inorg. Chem.* **1977**, *16*, 265.

0276-7333/87/2306-0799$01.50/0

Table I. Experimental Data for the X-ray Diffraction Study of $(\mu\text{-H})_2\text{Ru}_3(\mu_3\text{-}\eta^2\text{-CHC(O)OCH}_3)(\text{CO})_9$

(A) Unit Cell Data

a = 11.357 (3) Å
b = 12.427 (3) Å
c = 14.866 (4) Å
α = 73.989 (21)°
β = 69.581 (20)°
γ = 88.081 (20)°
V = 1885.4 (9) Å^3

cryst system: triclinic
space group: $P\bar{1}$ (C_i^1; No. 2)
Z = 4
formula: $C_{12}H_6O_{11}Ru_3$
mol wt 629.4
D(calcd) = 2.22 g cm^{-3}
T = 24 °C (297 K)

(B) Collection of X-ray Diffraction Data

diffractometer: Syntex $P2_1$
radiation: Mo Kα (λ = 0.710 730 Å)
monochromator: pyrolytic graphite; equatorial mode with 2θ(m) = 12.160° for the 002 reflection; assumed to be 50% perfect/50% ideally mosaic for polarization correction
reflctns measd: $+h,\pm k,\pm l$ for 2θ = 5.0 → 50.0°, yielding 6682 unique data (file name RUB3-219)
scan conditions: coupled θ(crystal)–2θ(counter) scan from $[2\theta(K\alpha_1) - 1.0]°$ through $[2\theta(K\alpha_2) + 1.0]°$ at 4.0 deg/min in 2θ
background measurement: stationary crystal and counter at each end of the 2θ scan; each for one-fourth of total scan time
std reflctns: three collected before each set of 97 data points; no decay observed
absorption correctn: μ(Mo Kα) = 23.7 cm^{-1}; corrected empirically by interpolation (in 2θ and ϕ) for 7 close-to-axial (ψ scan) reflections

group. Data were corrected for the effects of absorption (by interpolation, in 2θ and ϕ, between normalized curves from ψ scans of seven reasonably intense, close-to-axial, reflections) and were also corrected for Lorentz and polarization factors. Symmetry-equivalent data were averaged, and the resulting unique data set was placed on an approximately absolute scale by means of a Wilson plot.

Solution and Refinement of the Structure. All calculations were performed on the SUNY—Buffalo modified version of the Syntex XTL system. The analytical forms for the neutral atoms' scattering factors[7a] were corrected for both the real and imaginary components of anomalous dispersion.[7b] The function minimized during least-squares refinement was $\sum w(|F_o| - |F_c|)^2$, where $1/w = [\sigma(|F_o|)]^2 + [0.01|F_o|]^2$.

The structure was solved by direct methods using the program MULTAN,[8] the positions of the six independent ruthenium atoms being determined from an "E map". The remaining non-hydrogen and hydrogen atoms were located from difference-Fourier maps. Refinement of positional and thermal parameters of all non-hydrogen atoms, the hydride ligands, and the alkylidene hydrogens (with hydrogen atoms of the methyl group in idealized locations with d(C–H) = 0.95 Å[9]) led to convergence with[10] R_F = 3.2%, R_{wF} = 3.4%, and GOF = 1.45 for all 6682 unique data (R_F = 2.3% and R_{wF} = 3.1% for those 5586 data with $|F_o| > 6\sigma(|F_o|)$). A final difference-Fourier synthesis showed no unexpected features; the structure is thus both correct and complete. Final positional parameters are collected in Table II.

Table II. Final Atomic Coordinates for $(\mu\text{-H})_2\text{Ru}_3(\text{CO})_9(\mu_3\text{-}\eta^2\text{-CHC(O)OCH}_3)$

atom	x	y	z	B, Å^2
		Molecule A		
Ru(1A)	0.498 07 (3)	0.453 49 (3)	0.257 26 (2)	
Ru(2A)	0.472 42 (3)	0.680 93 (3)	0.184 81 (2)	
Ru(3A)	0.319 49 (3)	0.549 71 (3)	0.391 23 (2)	
O(1A)	0.321 25 (23)	0.626 87 (21)	0.150 07 (19)	
O(2A)	0.173 75 (26)	0.491 79 (23)	0.189 05 (23)	
O(11A)	0.779 12 (34)	0.480 42 (40)	0.222 72 (37)	
O(12A)	0.543 78 (39)	0.398 47 (32)	0.062 69 (25)	
O(13A)	0.452 79 (35)	0.205 19 (28)	0.373 84 (26)	
O(21A)	0.424 83 (41)	0.929 37 (29)	0.106 88 (31)	
O(22A)	0.670 28 (35)	0.742 90 (39)	0.257 77 (31)	
O(23A)	0.675 69 (34)	0.662 34 (34)	−0.007 52 (26)	
O(31A)	0.403 25 (42)	0.671 16 (31)	0.515 58 (28)	
O(32A)	0.232 90 (37)	0.335 44 (30)	0.563 96 (27)	
O(33A)	0.055 77 (31)	0.629 54 (33)	0.423 62 (30)	
C(1A)	0.300 22 (34)	0.465 34 (31)	0.288 83 (28)	
C(2A)	0.267 73 (33)	0.534 03 (31)	0.205 81 (28)	
C(3A)	0.136 66 (47)	0.557 52 (41)	0.107 52 (41)	
C(11A)	0.674 65 (48)	0.469 64 (42)	0.236 19 (37)	5.34 (10)
C(12A)	0.526 51 (41)	0.420 18 (37)	0.135 27 (33)	4.405 (81)
C(13A)	0.472 51 (41)	0.297 22 (40)	0.332 00 (34)	4.564 (83)
C(21A)	0.436 03 (41)	0.838 16 (40)	0.137 16 (34)	4.637 (84)
C(22A)	0.596 43 (45)	0.718 59 (40)	0.228 97 (35)	5.042 (91)
C(23A)	0.598 27 (42)	0.666 86 (37)	0.063 30 (34)	4.554 (84)
C(31A)	0.371 32 (42)	0.627 49 (39)	0.470 55 (34)	4.676 (85)
C(32A)	0.262 90 (41)	0.414 63 (38)	0.500 40 (33)	4.537 (83)
C(33A)	0.153 63 (42)	0.601 45 (37)	0.413 57 (32)	4.446 (82)
H(13A)	0.471 5 (44)	0.495 6 (40)	0.366 7 (35)	6.9 (12)
H(23A)	0.356 6 (36)	0.682 4 (32)	0.293 8 (29)	4.48 (91)
H(1A)	0.251 5 (34)	0.403 1 (31)	0.317 4 (27)	3.07 (78)
H(3A)	0.070 1	0.519 8	0.101 6	6.0
H(4A)	0.207 6	0.571 1	0.045 0	6.0
H(5A)	0.111 9	0.628 9	0.117 0	6.0
		Molecule B		
Ru(1B)	0.001 55 (3)	0.819 32 (3)	0.752 21 (2)	
Ru(2B)	0.007 11 (3)	1.009 83 (3)	0.813 18 (2)	
Ru(3B)	0.179 29 (3)	0.991 94 (3)	0.616 33 (2)	
O(1B)	0.152 76 (25)	0.933 30 (22)	0.864 61 (20)	
O(2B)	0.316 60 (28)	0.828 70 (25)	0.833 98 (24)	
O(11B)	−0.275 25 (30)	0.823 25 (37)	0.767 25 (31)	
O(12B)	−0.033 75 (38)	0.662 42 (29)	0.957 07 (24)	
O(13B)	0.069 17 (33)	0.641 65 (28)	0.639 33 (25)	
O(21B)	0.038 95 (43)	1.224 48 (34)	0.871 42 (39)	
O(22B)	−0.173 49 (35)	1.111 18 (35)	0.712 44 (29)	
O(23B)	−0.212 76 (34)	0.894 65 (31)	1.002 24 (25)	
O(31B)	0.106 58 (38)	1.190 33 (30)	0.473 50 (27)	
O(32B)	0.280 14 (37)	0.876 04 (36)	0.451 00 (29)	
O(33B)	0.435 59 (32)	1.085 75 (35)	0.593 99 (31)	
C(1B)	0.194 96 (36)	0.848 16 (33)	0.730 97 (29)	
C(2B)	0.217 99 (36)	0.873 38 (31)	0.813 22 (31)	
C(3B)	0.346 23 (55)	0.858 85 (49)	0.911 83 (47)	
C(11B)	−0.173 89 (44)	0.821 53 (38)	0.762 01 (34)	4.687 (86)
C(12B)	−0.025 70 (39)	0.720 05 (36)	0.881 99 (33)	4.246 (78)
C(13B)	0.041 73 (38)	0.705 38 (36)	0.681 96 (31)	4.079 (76)
C(21B)	0.033 35 (44)	1.145 95 (42)	0.849 36 (36)	5.130 (94)
C(22B)	−0.106 96 (43)	1.072 46 (39)	0.752 16 (34)	4.680 (86)
C(23B)	−0.127 51 (42)	0.934 59 (38)	0.932 39 (34)	4.527 (83)
C(31B)	0.133 15 (42)	1.118 14 (39)	0.525 51 (34)	4.721 (86)
C(32B)	0.245 90 (43)	0.918 10 (39)	0.512 84 (35)	4.844 (88)
C(33B)	0.341 41 (45)	1.053 28 (40)	0.599 17 (35)	4.961 (91)
H(13B)	0.014 0 (46)	0.914 8 (41)	0.652 0 (36)	7.6 (13)
H(23B)	0.125 9 (35)	1.071 2 (32)	0.704 8 (29)	4.55 (92)
H(1B)	0.255 6 (35)	0.794 7 (32)	0.705 6 (27)	3.64 (83)
H(3B)	0.417 1	0.823 5	0.921 4	6.0
H(4B)	0.275 2	0.836 4	0.973 9	6.0
H(5B)	0.361 1	0.938 5	0.894 7	6.0

Results and Discussion

Synthesis and Spectroscopic Characterization. Pyrolysis of $(\mu\text{-H})_3\text{Ru}_3(\mu_3\text{-CCO}_2\text{CH}_3)(\text{CO})_9$ in the absence of CO generates $(\mu\text{-H})_2\text{Ru}_3(\mu_3\text{-}\eta^2\text{-CHC(O)OCH}_3)(\text{CO})_9$ in moderate yield; heating the product for longer times causes decomposition to methyl acetate (34%) and a variety of metal-containing products, primarily $\text{Ru}_3(\text{CO})_{12}$.

The characterization of $(\mu\text{-H})_2\text{Ru}_3(\mu_3\text{-}\eta^2\text{-CHC(O)OCH}_3)(\text{CO})_9$ is straightforward. The molecular ion is observed in the EI mass spectrum. The spectroscopic characterization of $(\mu\text{-H})_2\text{Ru}_3(\mu_3\text{-}\eta^2\text{-CHC(O)OCH}_3)(\text{CO})_9$ in solution is consistent with the crystal structure (vide infra, Figure 2). The IR spectrum contains only terminal carbonyl stretches, and the presence of a coordinated acyl is indicated by the very low acyl stretching frequency (1540 cm^{-1}). The ^{1}H NMR spectrum clearly indicates that one hydride ligand has migrated to the methylidyne carbon,

---

(7) *International Tables for X-Ray Crystallography*; Kynoch: Birmingham, England, 1974; Vol. IV: (a) pp 99–101; (b) pp 149–150.

(8) Germain, G.; Main, P.; Woolfson, M. M. *Acta Crystallogr., Sect. A: Cryst. Phys., Diffr., Theor. Gen. Crystallogr.* **1971**, *A27*, 368.

(9) Churchill, M. R. *Inorg. Chem.* **1973**, *12*, 1213.

(10) R_F (%) = $100\sum||F_o| - |F_c||/\sum|F_o|$; R_{wF} (%) = $100[\sum w(|F_o| - |F_c|)^2/\sum w|F_o|^2]^{1/2}$; GOF = $[\sum w(|F_o| - |F_c|)^2/(\text{NO} - \text{NV})]^{1/2}$, where NO is the number of observations and NV is the number of variables.

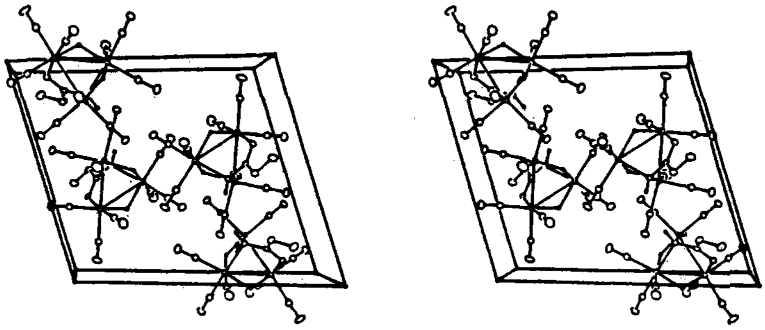

Figure 1. Packing of $(\mu\text{-H})_2\text{Ru}_3(\mu_3\text{-}\eta^2\text{-CHC(O)OCH}_3)(\text{CO})_9$ molecules within the triclinic unit cell of space group $P\bar{1}$. Here, $\vec{a}$ is toward the reader, $\vec{b}$ is obliquely down, and $\vec{c}$ is to the right (ORTEP diagram; 10% ellipsoids).

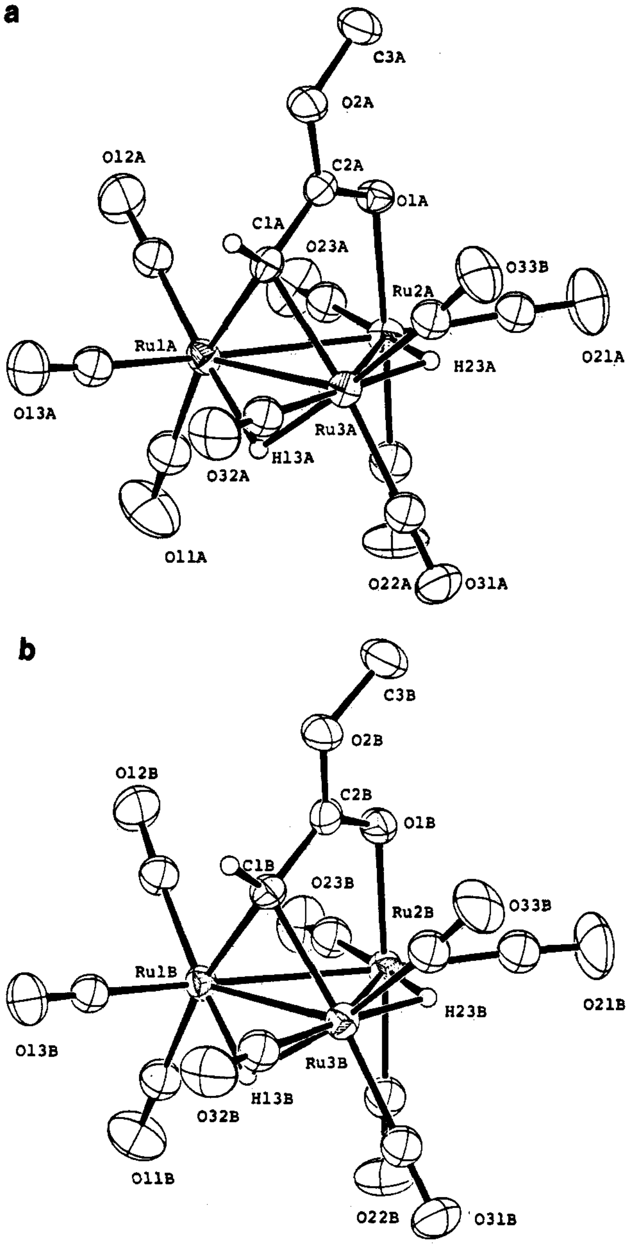

Figure 2. Labeling of atoms in the $(\mu\text{-H})_2\text{Ru}_3(\mu_3\text{-}\eta^2\text{-CHC(O)}\text{-}\text{OCH}_3)(\text{CO})_9$ molecules: (a) molecule A; (b) molecule B (ORTEP-II diagrams; 30% probability ellipsoids).

Table III. Interatomic Distances (Å) for $(\mu\text{-H})_2\text{Ru}_3(\mu_3\text{-}\eta^2\text{-CHC(O)OCH}_3)(\text{CO})_9$

molecule A		molecule B	
(A) Ru-Ru and Ru-H Distances			
Ru(1A)-Ru(2A)	2.778 (1)	Ru(1B)-Ru(2B)	2.768 (1)
Ru(1A)-Ru(3A)	2.800 (1)	Ru(1B)-Ru(3B)	2.795 (1)
Ru(2A)-Ru(3A)	2.967 (1)	Ru(2B)-Ru(3B)	2.962 (1)
Ru(1A)-H(13A)	1.77 (5)	Ru(1B)-H(13B)	1.59 (5)
Ru(3A)-H(13A)	1.79 (5)	Ru(3B)-H(13B)	1.97 (6)
Ru(2A)-H(23A)	1.70 (4)	Ru(2B)-H(23B)	1.70 (4)
Ru(3A)-H(23A)	1.82 (4)	Ru(3B)-H(23B)	1.79 (4)
(B) Distances Involving the μ_3-η^2-CHC(O)OCH$_3$ Ligand			
Ru(1A)-C(1A)	2.138 (4)	Ru(1B)-C(1B)	2.135 (4)
Ru(3A)-C(1A)	2.143 (4)	Ru(3B)-C(1B)	2.154 (4)
Ru(2A)-O(1A)	2.134 (3)	Ru(2B)-O(1B)	2.145 (3)
C(1A)-H(1A)	0.88 (4)	C(1B)-H(1B)	0.99 (4)
C(1A)-C(2A)	1.450 (5)	C(1B)-C(2B)	1.450 (6)
C(2A)-O(1A)	1.247 (5)	C(2B)-O(1B)	1.252 (5)
C(2A)-O(2A)	1.331 (5)	C(2B)-O(2B)	1.328 (5)
O(2A)-C(3A)	1.449 (6)	O(2B)-C(3B)	1.453 (7)
(C) Ru-CO Bond Lengths			
Ru(1A)-C(11A)	1.927 (6)	Ru(1B)-C(11B)	1.946 (5)
Ru(1A)-C(12A)	1.887 (5)	Ru(1B)-C(12B)	1.907 (4)
Ru(1A)-C(13A)	1.927 (5)	Ru(1B)-C(13B)	1.935 (5)
Ru(2A)-C(21A)	1.969 (5)	Ru(2B)-C(21B)	1.972 (5)
Ru(2A)-C(22A)	1.869 (5)	Ru(2B)-C(22B)	1.863 (5)
Ru(2A)-C(23A)	1.921 (5)	Ru(2B)-C(23B)	1.909 (5)
Ru(3A)-C(31A)	1.955 (5)	Ru(3B)-C(31B)	1.956 (5)
Ru(3A)-C(32A)	1.925 (5)	Ru(3B)-C(32B)	1.924 (5)
Ru(3A)-C(33A)	1.916 (5)	Ru(3B)-C(33B)	1.922 (5)
(D) C-O Distances			
C(11A)-O(11A)	1.138 (7)	C(11B)-O(11B)	1.126 (7)
C(12A)-O(12A)	1.134 (6)	C(12B)-O(12B)	1.122 (6)
C(13A)-O(13A)	1.128 (6)	C(13B)-O(13B)	1.117 (6)
C(21A)-O(21A)	1.119 (6)	C(21B)-O(21B)	1.122 (7)
C(22A)-O(22A)	1.148 (7)	C(22B)-O(22B)	1.132 (7)
C(23A)-O(23A)	1.126 (6)	C(23B)-O(23B)	1.144 (6)
C(31A)-O(31A)	1.121 (6)	C(31B)-O(31B)	1.121 (6)
C(32A)-O(32A)	1.124 (6)	C(32B)-O(32B)	1.128 (6)
C(33A)-O(33A)	1.125 (6)	C(33B)-O(33B)	1.125 (7)

and the two hydride resonances in the static spectrum at −10 °C are coupled to one another with a coupling constant of 3 Hz, the same as that found for $(\mu\text{-H})_2\text{Ru}_3(\mu_3\text{-}\eta^2\text{-MeC}_2\text{OMe})(\text{CO})_9$[1c] and other clusters of this class that contain hydrides bridging adjacent edges of the metal triangle. The ^{13}C NMR spectrum at −65 °C is listed in Table V, along with the most likely assignments (vide infra).[11] Although assignments of all of the carbonyl resonances cannot be made with certainty, the spectrum is clearly consistent with the 12-line spectrum expected for the solid-state structure if allowance is made for accidental overlap of three resonances.

Hydride Fluxionality. The molecule is fluxional at room temperature. The hydride resonances are exchange-broadened; a rough estimate of the rate constant for the exchange, 15 s^{-1}, was made from the line width at

---

(11) For comparison, the ^{13}C NMR spectrum of $(\mu\text{-H})_3\text{Ru}_3(\mu_3\text{-CCO}_2\text{Me})(\text{CO})_9$ consists of the following resonances (CDCl$_3$, 22 °C): 189.8 (3 C, axial carbonyls), 188.3 (6 C, equatorial carbonyls), 183.5 (1 C, acyl or methylidyne), 180.2 (1 C, acyl or methylidyne), and 52.6 (1 C, methyl) ppm.

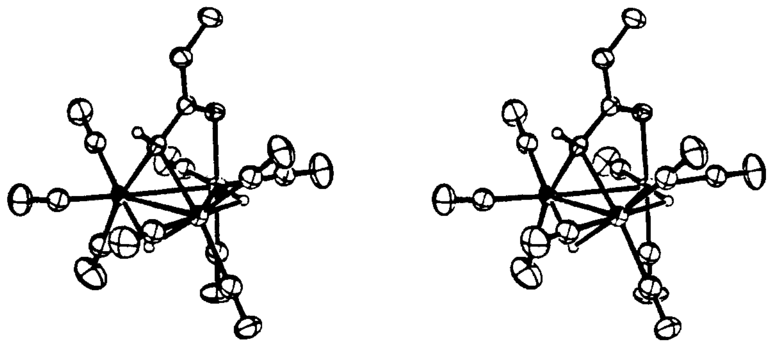

Figure 3. Stereoscopic view of $(\mu\text{-H})_2Ru_3(\mu_3\text{-}\eta^2\text{-CHC(O)OCH}_3)(CO)_9$, molecule A (ORTEP-II; 20% ellipsoids).

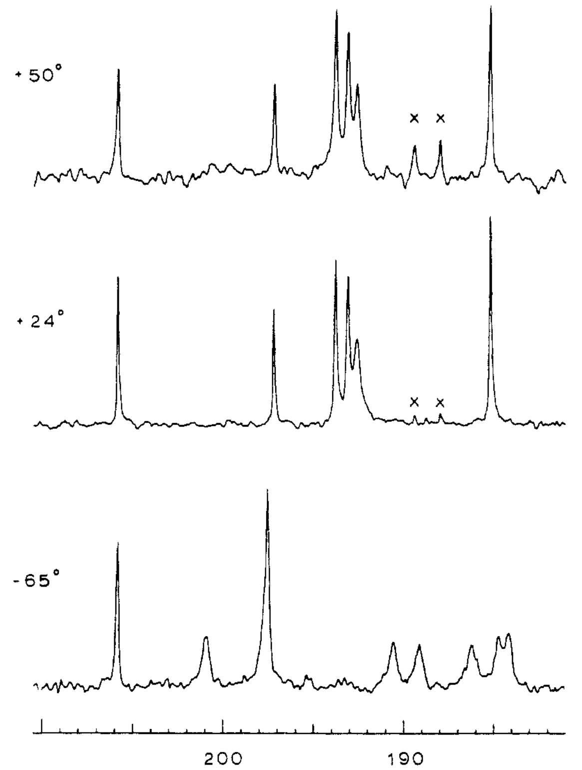

Figure 4. Variable-temperature ^{13}C NMR spectra for $(\mu\text{-H})_2Ru_3(\mu_3\text{-}\eta^2\text{-CHC(O)OCH}_3)(CO)_9$ in the carbonyl region. The two resonances marked with crosses are due to a decomposition product.

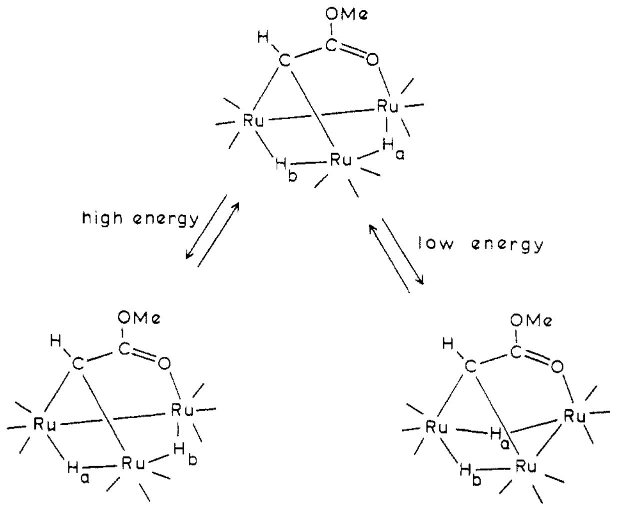

Figure 5. Proposed mechanisms for low-energy (a) and high-energy (b) fluxional processes.

299 K, corresponding to a free energy of activation of 66.5 kJ/mol (15.9 kcal/mol). The ^{13}C NMR spectrum also provides evidence for fluxional behavior (Figure 4). At 22 °C incomplete averaging of pairs of resonances, 201.1 and 184.8, 197.6 (1 C) and 190.5, 197.6 (1 C) and 189.2, and 186.3 and 184.2 ppm, occurs such that only six signals appear in the carbonyl region, 206.2 (1 C), 197.5 (1 C), 194.1 (2 C), 193.5 (2 C), 193.0 (br, 2 C), and 185.5 (2 C) ppm; the resonances due to the alkylidene and methyl carbons are essentially unchanged at 60.8 and 53.6 ppm. Increasing the temperature results in further sharpening of the exchange-averaged resonances. At the temperature of coalescence of the resonances at 201.1 and 184.8 ppm the rate constant for the exchange process is calculated to be 1600 s^{-1},[12] and since these lines have already coalesced at 22 °C, the process that averages the CO resonances in a pairwise manner is different from that which exchanges the hydride resonances and is much more facile ($\Delta G^{\ddagger} < 54$ kJ/mol (13 kcal/mol)). The most likely mechanism to account for these results is shown in Figure 5. The lowest energy process involves migration of hydride a to the unoccupied Ru–Ru edge, generating a plane of symmetry perpendicular to the Ru_3 plane and averaging CO ligands related by that symmetry but not exchanging the hydrides; at a slower rate hydrides a and b exchange, probably by initial migration of hydride b to the unoccupied Ru–Ru edge. Similar exchange processes have been reported for analogous $(\mu\text{-H})_2M_3(\mu_3\text{-}\eta^2\text{-L})(CO)_9$ clusters.[13]

Assignment of the resonances (Table V) in the carbonyl region can be attempted through the C–H coupling and the pairwise exchange predicted by the mechanism in Figure 5. The resonances due to carbonyls trans to hydride ligands should appear as doublets with coupling constants of ca. 10 Hz; three of the four expected resonances are observed, and the fourth is most likely one of the three overlapping lines of resonance (3) since this resonance decreases in intensity in the proton-coupled spectrum. The mechanism predicts that of the exchanging pairs one will be of two proton-coupled resonances, one will be of two

---

(12) At coalescence $k_c = 2^{1/2}\pi\Delta\nu$, where $\Delta\nu$ is the separation in hertz of the exchanging resonances in the absence of exchange: Wilkins, R. G. *The Study of Kinetics and Mechanism of Reactions of Transition Metal Complexes*; Allyn and Bacon: Boston, 1974; p 154.

(13) (a) Evans, J.; McNulty, G. S. *J. Chem. Soc., Dalton Trans.* **1981**, 2017. (b) Aime, S.; Deeming, A. J. *J. Chem. Soc., Dalton Trans.* **1983**, 1807. (c) Goudsmit, R. J.; Johnson, B. F. G.; Lewis, J.; Raithby, P. R.; Rosales, M. J. *J. Chem. Soc., Dalton Trans.* **1983**, 2257. (d) Jackson, W. G.; Johnson, B. F. G.; Lewis, J. *J. Organomet. Chem.* **1977**, *139*, 125. (e) Yin, C. C.; Deeming, A. J. *J. Chem. Soc., Dalton Trans.* **1982**, 2563. (f) Azam, K. A.; Yin, C. C.; Deeming, A. J. *J. Chem. Soc., Dalton Trans.* **1978**, 1201. (g) Azam, K. A.; Deeming, A. J.; Rothwell, I. P.; Hursthouse, M. B.; Backer-Dirks, J. D. J. *J. Chem. Soc., Dalton Trans.* **1981**, 2039. (h) Canty, A. J.; Domingos, A. J. P.; Johnson, B. F. G.; Lewis, J. *J. Chem. Soc., Dalton Trans.* **1973**, 2056. (i) Domingos, A. J. P.; Johnson, B. F. G.; Lewis, J. *J. Organomet. Chem.* **1972**, *36*, C43. (j) Jensen, C. M.; Kaesz, H. D. *J. Am. Chem. Soc.* **1983**, *105*, 6969. (k) Lavigne, G.; Lugan, N.; Bonnet, J.-J. *Organometallics* **1982**, *1*, 1040.

Table IV. Selected Interatomic Angles (deg) for $(\mu\text{-H})_2\text{Ru}_3(\mu_3\text{-}\eta^2\text{-CHC(O)OCH}_3)(\text{CO})_9$

(A) Internal Angles of the $(\mu\text{-H}_2)\text{Ru}_3$ Cores

Ru(3A)–Ru(1A)–Ru(2A)	64.26 (1)	Ru(1A)–H(13A)–Ru(3A)	104 (3)	Ru(3B)–Ru(1B)–Ru(2B)	64.34 (1)	Ru(1B)–H(13B)–Ru(3B)	103 (3)
Ru(1A)–Ru(2A)–Ru(3A)	58.23 (1)	Ru(2A)–H(23A)–Ru(3A)	115 (2)	Ru(1B)–Ru(2B)–Ru(3B)	58.26 (1)	Ru(2B)–H(23B)–Ru(3B)	117 (2)
Ru(2A)–Ru(3A)–Ru(1A)	57.51 (1)			Ru(2B)–Ru(3B)–Ru(1A)	57.40 (1)		

(B) Angles around the Ruthenium Atoms

Ru(2A)–Ru(1A)–C(1A)	75.67 (11)	O(1A)–Ru(2A)–H(23A)	83.6 (14)	Ru(2B)–Ru(1B)–C(1B)	75.83 (11)	O(1B)–Ru(2B)–H(23B)	85.5 (14)
Ru(2A)–Ru(1A)–C(11A)	95.54 (16)	C(21A)–Ru(2A)–C(22A)	93.54 (21)	Ru(2B)–Ru(1B)–C(11B)	96.51 (15)	C(21B)–Ru(2B)–C(22B)	94.18 (21)
Ru(2A)–Ru(1A)–C(12A)	95.52 (14)	C(21A)–Ru(2A)–C(23A)	98.96 (20)	Ru(2B)–Ru(1B)–C(12B)	93.50 (14)	C(21B)–Ru(2B)–C(23B)	99.09 (21)
Ru(2A)–Ru(1A)–C(13A)	165.00 (15)	C(21A)–Ru(2A)–H(23A)	84.7 (14)	Ru(2B)–Ru(1B)–C(13B)	164.10 (13)	C(21B)–Ru(2B)–H(23B)	83.9 (14)
Ru(2A)–Ru(1A)–H(13A)	80.1 (16)	C(22A)–Ru(2A)–C(23A)	91.05 (21)	Ru(2B)–Ru(1B)–H(13B)	79.3 (19)	C(22B)–Ru(2B)–C(23B)	90.92 (21)
C(1A)–Ru(1A)–C(11A)	168.78 (19)	C(22A)–Ru(2A)–H(23A)	91.7 (14)	C(1B)–Ru(1B)–C(11B)	169.90 (18)	C(22B)–Ru(2B)–H(23B)	88.6 (14)
C(1A)–Ru(1A)–C(12A)	93.66 (18)	C(23A)–Ru(2A)–H(23A)	175.3 (14)	C(1B)–Ru(1B)–C(12B)	90.21 (18)	C(23B)–Ru(2B)–H(23B)	177.1 (14)
C(1A)–Ru(1A)–C(13A)	91.29 (18)			C(1B)–Ru(1B)–C(13B)	91.45 (17)	C(1B)–Ru(3B)–C(31B)	169.89 (18)
C(1A)–Ru(1A)–H(13A)	85.7 (16)	C(1A)–Ru(3A)–C(31A)	169.12 (18)	C(1B)–Ru(1B)–H(13B)	91.9 (19)	C(1B)–Ru(3B)–C(32B)	93.01 (19)
C(11A)–Ru(1A)–C(12A)	94.13 (21)	C(1A)–Ru(3A)–C(32A)	91.14 (18)	C(11B)–Ru(1B)–C(12B)	96.90 (20)	C(1B)–Ru(3B)–C(33B)	90.16 (19)
C(11A)–Ru(1A)–C(13A)	96.40 (22)	C(1A)–Ru(3A)–C(33A)	91.35 (18)	C(11B)–Ru(1B)–C(13B)	94.89 (20)	C(1B)–Ru(3B)–H(13B)	81.9 (15)
C(11A)–Ru(1A)–H(13A)	86.0 (16)	C(1A)–Ru(3A)–H(13A)	85.1 (16)	C(11B)–Ru(1B)–H(13B)	80.1 (19)	C(1B)–Ru(3B)–H(23B)	90.7 (13)
C(12A)–Ru(1A)–C(13A)	92.65 (20)	C(1A)–Ru(3A)–H(23A)	90.5 (13)	C(12B)–Ru(1B)–C(13B)	96.10 (19)	C(31B)–Ru(3B)–C(32B)	91.55 (21)
C(12A)–Ru(1A)–H(13A)	175.6 (16)	C(31A)–Ru(3A)–C(32A)	92.82 (20)	C(12B)–Ru(1B)–H(13B)	171.8 (19)	C(31B)–Ru(3B)–C(33B)	98.51 (21)
C(13A)–Ru(1A)–H(13A)	91.7 (16)	C(31A)–Ru(3A)–C(33A)	98.49 (20)	C(13B)–Ru(1B)–H(13B)	91.8 (19)	C(31B)–Ru(3B)–H(13B)	89.2 (15)
Ru(1A)–Ru(2A)–O(1A)	85.12 (7)	C(31A)–Ru(3A)–H(13A)	85.1 (16)	Ru(1B)–Ru(2B)–O(1B)	84.94 (8)	C(31B)–Ru(3B)–H(23B)	85.3 (13)
Ru(1A)–Ru(2A)–C(21A)	174.21 (14)	C(31A)–Ru(3A)–H(23A)	86.7 (13)	Ru(1B)–Ru(2B)–C(21B)	173.10 (15)	C(32B)–Ru(3B)–C(33B)	94.13 (21)
Ru(1A)–Ru(2A)–C(22A)	91.22 (16)	C(32A)–Ru(3A)–C(33A)	93.80 (20)	Ru(1B)–Ru(2B)–C(22B)	90.11 (15)	C(32B)–Ru(3B)–H(13B)	88.5 (15)
Ru(1A)–Ru(2A)–C(23A)	84.22 (14)	C(32A)–Ru(3A)–H(13A)	85.5 (16)	Ru(1B)–Ru(2B)–C(23B)	86.22 (15)	C(32B)–Ru(3B)–H(23B)	175.0 (13)
Ru(1A)–Ru(2A)–H(23A)	91.9 (14)	C(32A)–Ru(3A)–H(23A)	173.9 (13)	Ru(1B)–Ru(2B)–H(23B)	90.9 (14)	C(33B)–Ru(3B)–H(13B)	171.8 (15)
O(1A)–Ru(2A)–C(21A)	89.85 (16)	C(33A)–Ru(3A)–H(13A)	176.4 (16)	O(1B)–Ru(2B)–C(21B)	90.20 (17)	C(33B)–Ru(3B)–H(23B)	82.5 (13)
O(1A)–Ru(2A)–C(22A)	173.94 (17)	C(33A)–Ru(3A)–H(23A)	80.3 (13)	O(1B)–Ru(2B)–C(22B)	172.26 (17)	H(13B)–Ru(3B)–H(23B)	95.4 (20)
O(1A)–Ru(2A)–C(23A)	93.38 (16)	H(13A)–Ru(3A)–H(23A)	100.5 (21)	O(1B)–Ru(2B)–C(23B)	94.69 (16)		

(C) Ru–C–O Angles

Ru(1A)–C(11A)–O(11A)	179.1 (5)	Ru(2A)–C(23A)–O(23A)	176.6 (4)	Ru(1B)–C(11B)–O(11B)	179.7 (5)	Ru(2B)–C(23B)–O(23B)	175.8 (4)
Ru(1A)–C(12A)–O(12A)	178.9 (4)	Ru(3A)–C(31A)–O(31A)	178.6 (5)	Ru(1B)–C(12B)–O(12B)	175.6 (4)	Ru(3B)–C(31B)–O(31B)	180.0 (5)
Ru(1A)–C(13A)–O(13A)	176.4 (4)	Ru(3A)–C(32A)–O(32A)	178.3 (4)	Ru(1B)–C(13B)–O(13B)	177.4 (4)	Ru(3B)–C(32B)–O(32B)	176.8 (5)
Ru(2A)–C(21A)–O(21A)	174.8 (5)	Ru(3A)–C(33A)–O(33A)	176.9 (4)	Ru(2B)–C(21B)–O(21B)	174.8 (5)	Ru(3B)–C(33B)–O(33B)	176.4 (5)
Ru(2A)–C(22A)–O(22A)	178.2 (5)			Ru(2B)–C(22B)–O(22B)	178.0 (5)		

(D) Angles within the $\mu_3\text{-}\eta^2\text{-CHC(O)OCH}_3$ Ligands

Ru(1A)–C(1A)–Ru(3A)	81.71 (14)	C(1A)–C(2A)–O(1A)	125.2 (4)	Ru(1B)–C(1B)–Ru(3B)	81.33 (15)	C(1B)–C(2B)–O(1B)	125.1 (4)
Ru(1A)–C(1A)–C(2A)	114.32 (27)	C(1A)–C(2A)–O(2A)	115.8 (3)	Ru(1B)–C(1B)–C(2B)	115.42 (29)	C(1B)–C(2B)–O(2B)	116.2 (4)
Ru(1A)–C(1A)–H(1A)	117.9 (26)	O(1A)–C(2A)–O(2A)	118.9 (4)	Ru(1B)–C(1B)–H(1B)	118.5 (24)	O(1B)–C(2B)–O(2B)	118.8 (4)
Ru(3A)–C(1A)–C(2A)	115.95 (27)	Ru(2A)–O(1A)–C(2A)	114.30 (24)	Ru(3B)–C(1B)–C(2B)	115.27 (29)	Ru(2B)–O(1B)–C(2B)	113.81 (26)
Ru(3A)–C(1A)–H(1A)	114.3 (26)	C(2A)–O(2A)–C(3A)	118.1 (4)	Ru(3B)–C(1B)–H(2B)	114.4 (23)	C(2B)–O(2B)–C(3B)	117.0 (4)
C(2A)–C(1A)–H(1A)	110.2 (26)			C(2B)–C(1B)–H(1B)	109.7 (24)		

noncoupled resonances, and two will be of one coupled and one noncoupled resonance. Thus, resonance (1) and one temperature-invariant line of resonance (3) are assigned to carbonyls j (or h) and h (or j) since these are not involved in any exchange process. The pair of exchanging coupled resonances ((5) and one of the carbonyls of resonance (3)) is assigned to carbonyls d and b. The pair of exchanging noncoupled resonances ((4) and one of the overlapping lines of resonance (3)) is assigned to carbonyls f and g. Of the remaining exchanging pairs the one having the greatest difference in chemical shifts, (2) and (7), is assigned to the pair on the Ru atom to which the acyl is coordinated, a and i, respectively, since the differences in the chemical shifts of the members of the other exchanging pairs, which must be on the two Ru atoms bridged by the alkylidene carbon, are much smaller. Then resonances (6) and (8) are assigned to carbonyls e and c, respectively.

Crystal Structure and Molecular Geometry of $(\mu\text{-H})_2\text{Ru}_3(\mu_3\text{-}\eta^2\text{-CHC(O)OCH}_3)(\text{CO})_9$. $(\mu\text{-H})_2\text{Ru}_3(\mu_3\text{-}\eta^2\text{-CHC(O)OCH}_3)(\text{CO})_9$ is the first triruthenium alkylidene of the class of clusters having the general formula $(\mu\text{-H})_2\text{M}_3(\mu_3\text{-}\eta^2\text{-L})(\text{CO})_9$,[1c,13-17] where L is alkyne, *o*-phenylene, vinylidene, or another five-electron donor and M is Ru or Os. Several osmium alkylidenes of this general formulation have been reported. Representative examples are $(\mu\text{-H})_2\text{Os}_3(\mu_3\text{-}\eta^2\text{-PhCCH=O})(\text{CO})_9$ (coordinated acyl),[14] $(\mu\text{-H})_2\text{Os}_3(\mu_3\text{-}\eta^2\text{-OC}_6\text{H}_3\text{CH}_2\text{Ph})(\text{CO})_9$ (coordinated ketone, structurally characterized),[15] $(\mu\text{-H})_2\text{Os}_3(\mu_3\text{-}\eta^2\text{-Me}_2\text{PCH})(\text{CO})_9$ (coordinated phosphorus),[16] and $(\mu\text{-H})_2\text{Os}_3(\mu_3\text{-}\eta^2\text{-MeCOMe})(\text{CO})_9$ (coordinated ether).[17] Other methylene-containing Ru$_3$ clusters previously reported are $\text{Ru}_3(\eta^3\text{-}(C,C,O),\ \mu_3\text{-COCH}_2)(\mu\text{-CH}_2)(\text{CO})_7(\text{dppm})$,[18] $\text{Ru}_3(\mu\text{-CH}_2)$(1,4-dineopentyl-1,4-diaza-1,3-butadiene)$(\text{CO})_8$,[19] $\text{Ru}_3(\mu\text{-CH}_2)(\mu_3\text{-}\eta^2\text{-CH}_2\text{CC-}i\text{-Pr})(\mu\text{-PPh}_2)(\text{CO})_7$,[20] and $\text{Ru}_3(\mu\text{-CO})(\mu\text{-CH}_2)(\text{CO})_{10}$.[21] However, $(\mu\text{-H})_2\text{Ru}_3(\mu_3\text{-}\eta^2\text{-CHC(O)OCH}_3)(\text{CO})_9$ is the first such cluster prepared by a reductive elimination of a C–H bond. Because of the importance of this product as a potential intermediate in the reductive elimination process and because previous structural studies of analogous Os clusters have not located the hydride ligands, we undertook a X-ray crystallographic investigation of $(\mu\text{-H})_2\text{Ru}_3(\mu_3\text{-}\eta^2\text{-CHC(O)OCH}_3)(\text{CO})_9$.

---

(14) Azam, K. A.; Deeming, A. J.; Rothwell, I. P. *J. Chem. Soc., Dalton Trans.* **1981**, 91.

(15) Azam, K. A.; Deeming, A. J.; Rothwell, I. P.; Hursthouse, M. B.; New, L. *J. Chem. Soc., Chem. Commun.* **1978**, 1086.

(16) Deeming, A. J.; Underhill, M. *J. Chem. Soc., Dalton Trans.* **1973**, 2727.

(17) Boyar, E.; Deeming, A. J.; Arce, A. J.; De Sanctis, Y. *J. Organomet. Chem.* **1984**, *276*, C45.

(18) Holmgren, J. S.; Shapley, J. R.; Wilson, S. R.; Pennington, W. T. *J. Am. Chem. Soc.* **1986**, *108*, 508.

(19) Keijsper, J.; Polm, L. H.; van Koten, G.; Vrieze, K.; Goubitz, K.; Stam, C. H. *Organometallics* **1985**, *4*, 1876.

(20) Nucciarone, D.; Taylor, N. J.; Carty, A. J. *Organometallics* **1984**, *3*, 177.

(21) Holmgren, J. S.; Shapley, J. R. *Organometallics* **1985**, *4*, 793.

Table V. ^{13}C NMR Assignments for $(\mu\text{-}H)_2Ru_3(\mu_3\text{-}\eta^2\text{-}CHC(O)OCH_3)(CO)_9$

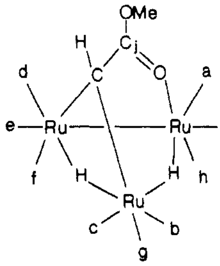

resonance[a]	assignt
(1) 205.8 (1 C)	j (or h)
(2) 201.1 (1 C)[b]	a (or c)
(3) 197.6 (3 C)[c]	h (or j) d (or b) g (or f)
(4) 190.5 (1 C)	f (or g)
(5) 189.2 (1 C)[d]	b (or d)
(6) 186.3 (1 C)	e (or i)
(7) 184.8 (1 C)	i (or e)
(8) 184.2 (1 C)[c]	c (or a)
(9) 60.0 (1 C)[e]	alkylidene
(10) 54.0 (1 C)[f]	methyl

[a] Chemical shift in ppm relative to $CDCl_3$ (77.2 ppm). [b] J_{CH} = 11 Hz. [c] Unresolved coupling to hydrogen. [d] J_{CH} = 10 Hz. [e] J_{CH} = 145 Hz. [f] J_{CH} = 148 Hz.

The crystal consists of discrete molecular units of $(\mu\text{-}H)_2Ru_3(\mu_3\text{-}\eta^2\text{-}CHC(O)OCH_3)(CO)_9$, which are mutually separated at normal van der Waals' distances; there are no abnormally short intermolecular contacts. There are two independent molecules in the asymmetric unit. The triclinic unit cell contains four molecules; the packing arrangement is illustrated in Figure 1. Each molecule is chiral, but the crystal contains an ordered racemic mixture of the two enantiomers by virtue of the crystallographic inversion centers. The two molecules are structurally equivalent and their labeling schemes are given in Figure 2. A stereoview of molecule A appears as Figure 3. Interatomic distances and angles are collected in Tables III and IV such that equivalent values for molecules "A" and "B" appear side by side. The following discussion will refer to bond lengths and angles in molecule A, with equivalent values for molecule B following in square brackets. Average values will include parameters from both molecules.

The complex is based upon a triangular array of ruthenium atoms. The shortest ruthenium–ruthenium bond length occurs for the unsupported metal–metal bond with Ru(1)–Ru(2) 2.778 (1) Å [2.768 (1) Å], a value somewhat reduced from Ru–Ru(average) = 2.854 (5) Å in the parent compound $Ru_3(CO)_{12}$.[22] The μ-hydrido–μ-alkylidene-bridged linkage has an intermediate value with Ru(1)–Ru(3) = 2.800 (1) Å [2.795 (1) Å], a value similar to those observed previously for the Ru(μ-H)(μ-C)Ru systems in $(\mu\text{-}H)Ru_3(\mu\text{-}CNMe_2)(CO)_{10}$ (2.7997 (5) and 2.8016 (6) Å for two independent molecules)[23] and $(\mu\text{-}H)Ru_3(\mu\text{-}COMe)(CO)_{10}$ (2.821 (1) Å);[24] a comparison with further $(\mu\text{-}H)Ru_3(\mu\text{-}X)(CO)_{10}$ systems is given in Table VII of ref 1d.

The longest intermetallic distance is observed for the equatorially hydrido-bridged Ru–Ru bond, Ru(2)–Ru(3) = 2.967 (1) Å [2.962 (1) Å]. Such an expansion of an equatorially hydrido-bridged M–M distance relative to a nonbridged M–M bond length is well-documented[23] and is particularly well-illustrated in a comparative study of the isomorphous clusters $(\mu\text{-}H)(H)Os_3(CO)_{11}$ and $Os_3(CO)_{12}$.[25]

The $\mu_3\text{-}\eta^2\text{-}CHC(O)OCH_3$ ligand lies over the triruthenium core. Atom C(1) represents the α-carbon of an alkylidene fragment and bridges Ru(1) and Ru(3) with Ru(1)–C(1) = 2.138 (4) Å [2.135 (4) Å], Ru(3)–C(1) = 2.143 (4) Å [2.154 (4) Å], and Ru–C(1)(average) = 2.143 ± 0.008 Å. The C(1)–C(2) distance is 1.450 (5) Å [1.450 (6) Å] and is reduced slightly from the accepted C(sp^3)–C(sp^2) single bond length of 1.510 ± 0.005 Å.[26] The C(2)–O(1) bond is essentially a carbon–oxygen double bond with d[C(2)–O(1)] = 1.247 (5) Å [1.252 (5) Å], a value expanded slightly from the tabulated[26] value of 1.233 ± 0.005 Å for the C═O bond length in carboxylic acids and esters. The C–OCH$_3$ bond is significantly longer than this, with C(2)–O(2) = 1.331 (5) Å [1.328 (5) Å]—again, marginally longer than the value of 1.312 ± 0.005 Å[26] accepted for the longer bond in carboxylic acids and esters. Finally, the bridge across the triruthenium cluster is completed by a donor O:→Ru linkage, in which Ru(2)–O(1) = 2.134 (3) Å [2.145 (3) Å].

Each ruthenium atom is linked to three terminal carbonyl ligands with Ru–CO bond lengths ranging from 1.869 (5) through 1.969 (5) Å [1.863 (5)–1.972 (5) Å]. The shortest Ru–CO distance is for the carbonyl ligand trans to the coordinated oxygen atom of the ester group, i.e., Ru(2)–C(22) = 1.869 (15) Å [1.863 (5) Å]; this presumably reflects a lack of competition for π-electron donation from Ru(2) to O(1) as compared to that for the C(22)–O(22) ligand. The longest Ru–CO linkage is for the carbonyl ligand on Ru(2) trans to the direct Ru–Ru linkage, i.e., Ru(2)–C(21) = 1.969 (5) Å [1.972 (5) Å]. This is slightly longer than the analogous linkage to Ru(1) at the other end of the linear OC–Ru(1)–Ru(2)–CO system, Ru(1)–C(13) = 1.927 (5) Å [1.935 (5) Å], perhaps because of the different coordination of environment of Ru(2) relative to Ru(1) (particularly the presence of the σ-donating and possibly *π-donating* oxygen atom, O(1), on Ru(2). Other Ru–CO distances are such that those trans to hydride ligands lie in the range 1.887 (5)–1.925 (5) Å [1.907 (4)–1.924 (5) Å] and are marginally shorter than those trans to the alkylidene carbon (C(1)), with Ru–CO = 1.927 (6)–1.955 (5) Å [1.946 (5)–1.956 (5) Å]. The pattern is blurred slightly because of each ruthenium atom being in a different coordination environment.

The hydride ligands were located and refined. Although the associated Ru–H distances are of limited precision and show substantial variations (i.e., Ru–H = 1.70 (4)–1.82 (4) Å [1.59 (5)–1.97 (6) Å], with an average value of 1.77 ± 0.11 Å), the essential stereochemical locations are internally consistent and definite. Thus, H(13) occupies a "semiaxial" bridging position between Ru(1) and Ru(3), in a site equivalent to that occupied by the alkylidene carbon, C(1). Atom H(23) occupies an diequatorial site in the plane of the Ru$_3$ cluster and bridges Ru(2) and Ru(3).

If we ignore direct Ru–Ru interactions in the hydrido-bridged Ru(1)–Ru(3) and Ru(2)–Ru(3) systems, then each ruthenium atom has an approximately octahedral coordination environment. That of Ru(2) lies strictly axial and equatorial relative to the triruthenium system, whereas those of Ru(1) and Ru(3) are canted in the disrotatory

---

(22) Churchill, M. R.; Hollander, F. J.; Hutchinson, J. P. *Inorg. Chem.* **1977**, *16*, 2655.

(23) Churchill, M. R.; DeBoer, B. G.; Rotella, F. J. *Inorg. Chem.* **1976**, *15*, 1843.

(24) Churchill, M. R.; Beanan, L. R.; Wasserman, H. J.; Bueno, C.; Rahman, Z. A.; Keister, J. B. *Organometallics* **1983**, *2*, 1179.

(25) Churchill, M. R.; DeBoer, B. G. *Inorg. Chem.* **1977**, *16*, 878. See also the related study on $(\mu\text{-}H)(H)Os_3(CO)_{10}(PPh_3)$; Churchill, M. R.; DeBoer, B. G. *Inorg. Chem.* **1977**, *16*, 2397.

(26) *Spec. Publ.—Chem. Soc.* **1965**, *No. 18*, S15s, S20s, S21s.

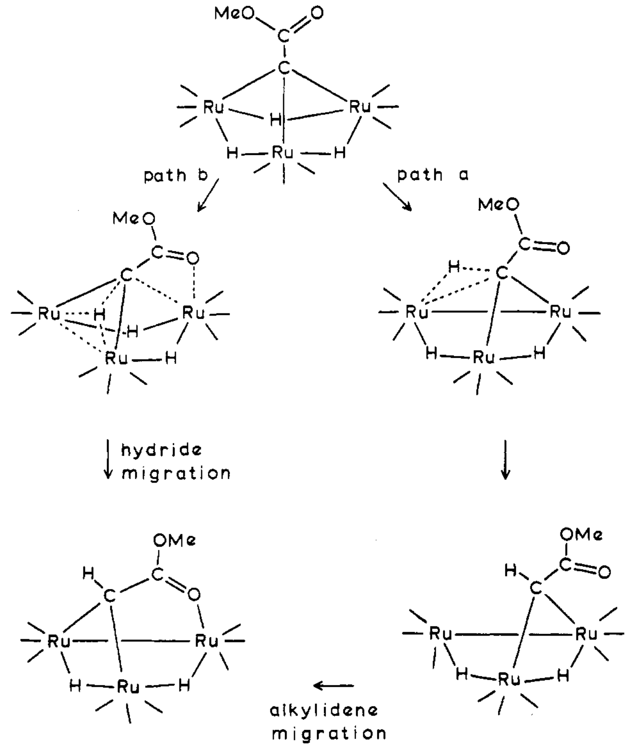

Figure 6. Possible mechanisms for rearrangement of $(\mu\text{-}H)_3Ru_3(\mu_3\text{-}CC(O)OCH_3)(CO)_9$ to $(\mu\text{-}H)_2Ru_3(\mu_3\text{-}\eta^2\text{-}CHC(O)OCH_3)(CO)_9$.

fashion so as to enable atoms C(1) and H(13) to occupy sites common to both octahedra.

Reductive Elimination of Methyl Acetate. Pyrolysis of $(\mu\text{-}H)_3Ru_3(\mu_3\text{-}CCO_2CH_3)(CO)_9$ in the absence of CO generates $(\mu\text{-}H)_2Ru_3(\mu_3\text{-}\eta^2\text{-}CHC(O)OCH_3)(CO)_9$ in moderate yield; heating the product for longer times causes decomposition to methyl acetate (34%) and a variety of Ru-containing products, primarily $Ru_3(CO)_{12}$. In the presence of CO $(\mu\text{-}H)_2Ru_3(\mu_3\text{-}\eta^2\text{-}CHC(O)OCH_3)(CO)_9$ is not detected, only methyl acetate (>80%) and $Ru_3(CO)_{12}$ are formed. However, the first-order rate constant for disappearance of the starting material is the same for both cases ($\Delta H^\ddagger = 111$ (±1) kJ/mol (26.6 (± 0.3) kcal), $\Delta S^\ddagger = -0.8$ (± 4) J/(degmol) (−0.2 (± 0.9) eu), and $k = 7.9 \times 10^{-5}$ s^{-1} at 70 °C), implying the same rate-determining step.[27] Under a CO atmosphere the pseudo-first-order rate constant for decomposition of $(\mu\text{-}H)_2Ru_3(\mu_3\text{-}\eta^2\text{-}CHC(O)OCH_3)(CO)_9$ is 1.0×10^{-4} s^{-1} at 70.5 °C, slightly larger than the rate constant for the first step. Thus, $(\mu\text{-}H)_2Ru_3(\mu_3\text{-}\eta^2\text{-}CHC(O)OCH_3)(CO)_9$ could be an intermediate in the conversion of $(\mu\text{-}H)_3Ru_3(\mu_3\text{-}CCO_2CH_3)(CO)_9$ to methyl acetate and ruthenium carbonyls; alternatively, both reactions may share a common, unsaturated intermediate that is intercepted by CO to produce methyl acetate or, in the absence of CO, is stabilized by coordination of the acyl.

At this point the mechanism of the rearrangement is still unclear. The low value for the enthalpy of activation, relative to values for reductive elimination of CH_3X from $(\mu\text{-}H)_3Ru_3(\mu_3\text{-}CX)(CO)_9$ (X = Ph ($\Delta H^\ddagger = 131$ kJ/mol (31.4 kcal)) and Cl ($\Delta H^\ddagger = 131$ kJ/mol (31.4 kcal))) may indicate direct involvement of the acyl group in the rate-determining step.[3] Since the acyl substituent should be oriented away from the developing unsaturated metal center during the reductive elimination step (path a, Figure 6), it is difficult to imagine how this participation might occur, but one possibility is shown in path b of Figure 6. Studies of the mechanism of this rearrangement and the subsequent reaction with CO are now in progress and will be the subject of a later paper.

Stabilization of $(\mu\text{-}H)_2Ru_3(\mu_3\text{-}\eta^2\text{-}CHC(O)OCH_3)(CO)_9$ after reductive elimination of a single C–H bond is achieved by coordination of the two-electron donor acyl moiety. In the next paper we will show that when the methylidyne substituent has the ability to act as a four-electron donor, two C–H bonds may be formed and a stabilized alkyl-containing cluster is thus produced.[28]

Acknowledgment. This work was supported by the National Science Foundation through Grant CHE85-20276 to J.B.K.

Supplementary Material Available: A table of anisotropic thermal parameters (1 page); a listing of structural factors (32 pages). Ordering information is given on any current masthead page.

---

[27] Duggan, T. P.; Keister, J. B., unpublished results.

[28] Churchill, M. R.; Ziller, J. W.; Dalton, D. M.; Keister, J. B., *Organometallics*, following paper in this issue.